ROSS, V.E. and VAN DEVENTER, J.S.J. A computer model to predict froth behaviour in the scale-up of flotation cells. APCOM 87. Proceedings of the Twentieth International Symposium on the Application of Computers and Mathematics in the Mineral Industries. Volume 2: *Metallurgy*. Johannesburg, SAIMM, 1987. pp. 73 – 88.

A Computer Model to Predict Froth Behaviour in the Scale-up of Flotation Cells

V.E. ROSS* and J.S.J. VAN DEVENTER**

**Ore-Dressing Division, Mintek, Randburg and **Department of Metallurgy, University of Stellenbosch, Stellenbosch, South Africa*

A computer program was developed that incorporates a novel analysis of the behaviour of the froth in full-scale cells to predict the performance of the froth over a wide range of operating conditions. The program has the distinct advantage that it can be easily implemented on a microcomputer, which allows rapid computation and processing of the results.

The program utilizes experimental data obtained in flotation-plant and laboratory testwork to provide parameters for the froth model under an initial set of operating conditions. These parameters can then be used in conjunction with a model describing the transfer of material from the pulp to the froth to predict the performance of the cell when its dimensions and operating variables are changed during scale-up.

Introduction

The scale-up of flotation cells from the laboratory to an industrial scale is complicated by several factors, particularly those relating to the effects of the structure and the residence time of the froth.[1-4] These complications are due to significant differences in the dimensions of the cells, in the operating conditions, such as the depth of the froth and the aeration rate, and in the methods of froth removal.

The flotation rate constants are closely related to the rate of aeration,[2] the extent to which the surfaces of the bubbles are covered by floating particles,[5] and the height of the froth column.[6] On a laboratory scale, the residence time of mineral particles in the froth is extremely short, owing to the rapid removal of the froth. On a plant scale, however, the longer residence times have a significant effect on the recovery of and selectivity for any particular species.

Hitherto, the prediction of the performance of large-scale flotation cells from batch data was accomplished by the implementation of a scale-up factor of between 1,5 and 3,5, i.e. the ratio of the residence time in a full-scale cell to that in a laboratory-scale cell, while the contribution of froth effects was totally neglected.[7,8] However, the method has limited application, since the laboratory and plant flotation rate constants are based on a specific set of operating conditions.

A computer program, which utilizes

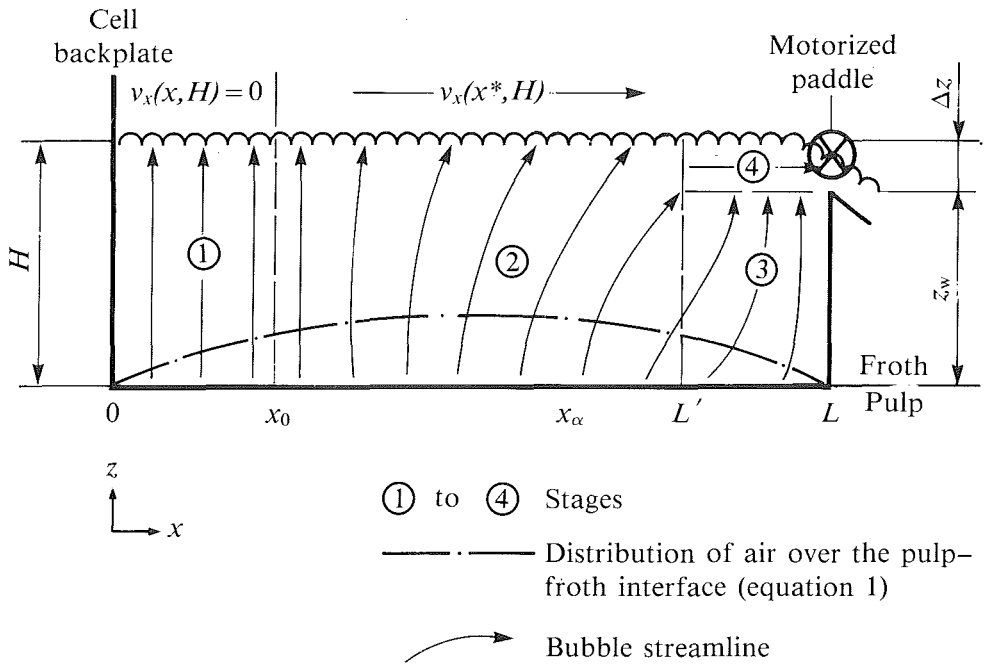

H	Total froth height, m
L	Length of flotation cell, m
L'	Right-hand boundary of stage 2 (distance from cell backplate), m
$v_x(x,H)$	Horizontal velocity of the froth at the surface, m/s
x	Distance from cell backplate, m
x_0	Right-hand boundary of stage 1 (distance from cell backplate), m
x_α	Origin of bubble streamline corresponding to (L', z_w), m
x^*	Distance from the right-hand boundary of stage 1, m
z_w	Height of concentrate weir above the pulp–froth interface, m
Δz	Height at which concentrate overflows concentrate weir, m

FIGURE 1. Schematic representation of the froth phase

a mathematical model of the froth phase as well as experimental flotation data to predict the performance of an industrial-scale froth, is described. It takes the characteristics of the froth into account during scale-up since they can cause significant deviations from predicted performance when only the residence time of the pulp has been considered.

The model

In the model developed in the present work, the froth phase is subdivided into four stages, which are indicated by the circled numbers in Figure 1. Stage 1 represents the inefficient part of the total froth volume,[9] i.e. the part that does not contribute towards the transfer of particles from the pulp into the concentrate stream. The relative size of this stagnant region is determined by tests in which small polystyrene beads are sprinkled onto the surface of the froth to indicate its velocity. Plug flow is assumed here, since no froth is transferred from this stage to any other stage.

A fraction ϵ of the total volume of air, G_t, flowing into the cell is transferred into stages 2 and 3 via the pulp-froth interface. Of this

air, a fraction ß is transferred into stage 2. The distribution of the air over the pulp-froth interface can be described by an equation of the form

$$(g_0)_x = g_0 \sin \pi x/L \qquad [1]$$

where $(g_0)_x$ is the superficial air flux at a distance x from the cell backplate, g_0 is the air flux at the centre of the cell, and L is the length of the cell.

This form of equation was verified by measurement of the air distribution in plant-scale cells with apparatus specifically designed for this purpose. A model of the froth phase by Moys,[9] which can predict concentrate flowrates only if the air distribution is independent of the distance from the cell backplate, can therefore not be applied in this case.

In stage 2, froth flow patterns can be observed in the direction of the froth discharge launder, i.e. the bubble velocity has both vertical (z) and horizontal (x) components. These bubble streamlines can be described by modification of the equation for an incompressible fluid flowing round a rectangular bend, to give:

$$x^* (F_1 + z_w - z) = c_2 = x^* (c_1 - z) \qquad [2]$$

where x^* is the distance from the right-hand boundary of stage 1 ($x = x_0$ in Figure 1), F_1 is a characteristic constant (m) that is calculated from the surface velocity of the froth (measured on the plant in tests using small polystyrene beads) and the volume of air and slurry transferred across the pulp-froth interface into the froth, and c_2 is a characteristic constant (m^2) for every bubble streamline. As the surface velocity of the froth in stage 2 is largely determined by the rate of concentrate removal, F_1 is a function of the rotational speed of the froth paddles.

The bubble velocity (m/s) at any coordinate (x^*,z) is

$$V(x^*,z) = V(x_s^*,0) \cdot \sqrt{\frac{x^{*2} + (c_1 - z)^2}{x_s^{*2} + c_1^2}} \qquad [3]$$

where $V(x_s^*,0)$ is the bubble velocity (m/s) at the pulp-froth interface at a distance x_s^* into stage 2, i.e.

$$V(x_s^*,0) = (g_0)_{x_s^*} (1 + \text{SLAR}) \qquad [4]$$

where SLAR is the ratio of the volumetric flowrate of the solids and water to that of the air as they enter the froth, as determined in laboratory testwork.

A fraction α of the air entering stage 2 at the interface between x_0 and L' is transferred into stage 3 at $x = L'$ between the boundaries $z = 0$ and $z = H$. The value of L' is determined by an iterative procedure from the calculated residence time of the froth in stage 3 (see the Addendum, Section 2).

The froth is transferred into stage 3 via stage 2 and via the pulp-froth interface. As a result, the vertical upward velocity of the

froth increases with increasing height above the interface:

$$V_3(z) = a_3 + \frac{g_0 L}{\pi}\left\{\cos\pi\left[\frac{L'}{L} - \frac{z(L' - x_\alpha)}{z_w L}\right] - \cos\pi\frac{L'}{L}\right\}/L_3 \qquad [5]$$

where

$a_3 = (1-\beta)(1+\mathrm{SLAR})\epsilon G_t/A_3$, (m/s),
$L_3 = L - L'$ (m)
$A_3 = L_3 W$ (m^2)
$g_0 = G_t\pi/2A_c$, the air flux at the centre of the cell,
x_α = the origin of the bubble streamline corresponding to (L', z_w), distance from the cell backplate,
A_c = cross-sectional cell area,
z_w = height (m) of the concentrate weir above the pulp-froth interface.

The froth is transferred into stage 4 from stage 2 as well as from stage 3. The horizontal velocity of the froth increases linearly towards the froth discharge (the magnitude of which increases with an increase in the rate of concentrate removal) and can be described by the relationship:

$$V_4(x) = a_4 + b_4(x - L') \qquad [6]$$

where $a = V(L', H - \Delta z/2)$

$$b = [V_3(z_w)A_3 - W\int_{L'}^{L}(g_{b0} + 2g_{b1}x)dx]/\Delta z A_3 \quad (\text{in } s^{-1}),$$

Δz is the height (m) at which the concentrate overflows the weir, and

g_{b0} (m/s) and g_{b1} (s^{-1}) are parameters describing bubble breakage at the froth surface.

The volumetric flowrate of the concentrate is then

$$Q_c = \bar{\bar{V}}(L, H - \Delta z/2)\Delta z W, \ (m^3/s), \qquad [7]$$

where $\bar{\bar{V}}(L, H - \Delta z/2)$ is the average velocity of the concentrate overflowing the concentrate weir.

The equations describing the concentrations of floated or entrained mineral particles, or both, and water in stage 2 are based on the assumption of first-order kinetics (see the Addendum, Section 1). The same assumption applies to all the other stages. The equations for stages 3 and 4 can be derived by incorporation of the velocity profiles given in Equations [5] and [6], but they are too complex to be described within the confines of this paper.

The drainage velocity (m/s) of any species at the left-hand boundary of stage 2 is[10]

$$U_i(x_0, z) = \Delta V_i - V(x_0, z), \qquad [8]$$

where ΔV_i is the velocity increment between the bubble and the drainage velocity (unique to species i), and $V(x_0, z)$ is the magnitude of the bubble velocity at (x_0, z).

The velocity increment is calculated from the total concentration of species i in the froth at $(x_0, 0)$, and is used in the calculation of the total concentration of the various species in the froth.

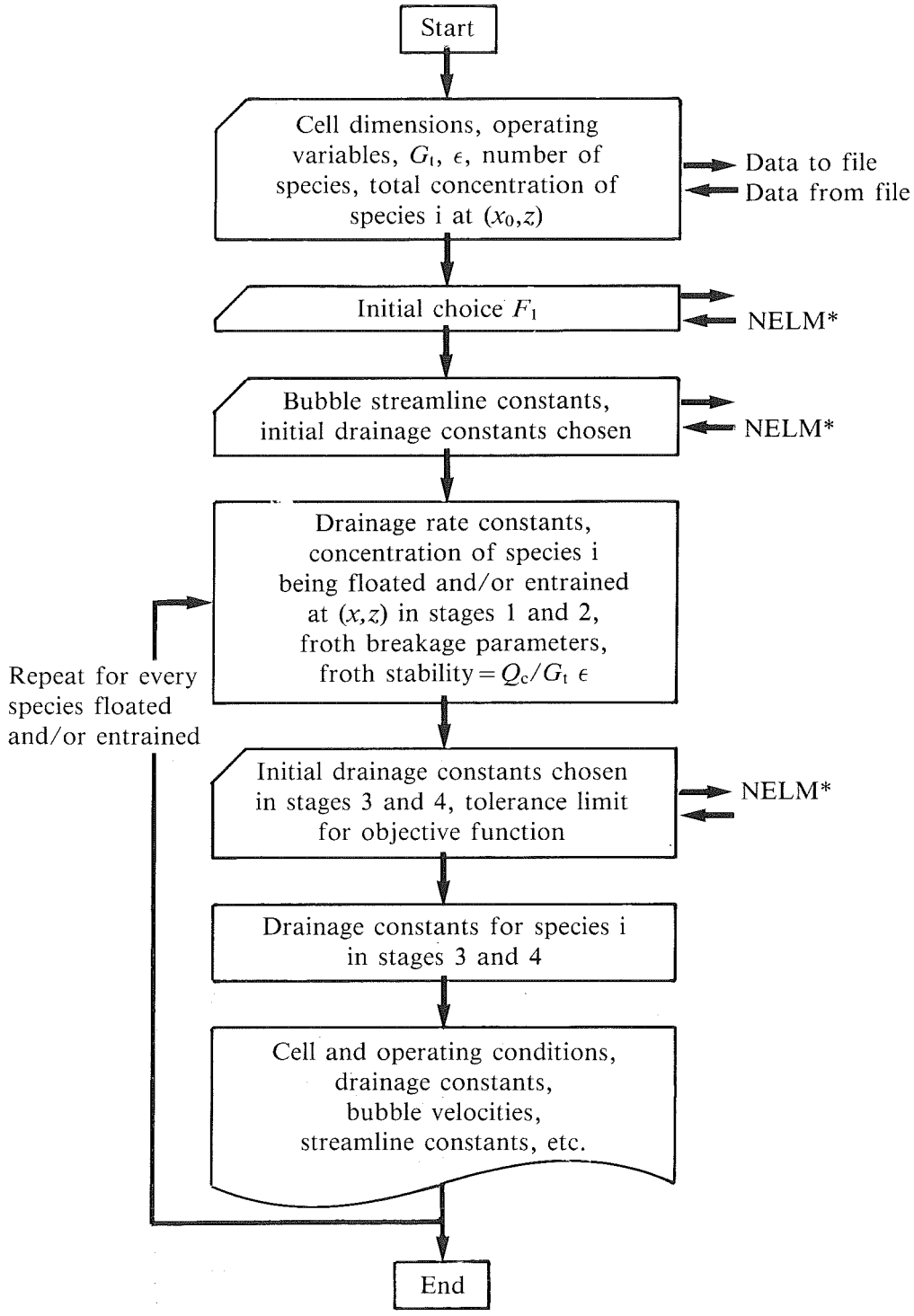

* Nelder–Mead optimization routine

FIGURE 2. Simplified flowsheet of the computational procedure SIMULATE

Computer requirements

A distinct advantage of the computer program is that it can be implemented with ease on a microcomputer. This is particularly important when access to a mainframe is not readily available. The program itself occupies less that 40 kilobytes of disc storage space, the computation time being typically about 5 minutes for the complete analysis of the behaviour of one

mineral species in the froth.

The computer program was developed on an Olivetti M24 microcomputer with 640 kilobytes of RAM storage capacity, using an MS-DOS operating system. GWBASIC was used as the programming language. A considerable degree of user-friendliness, which improves the versatility of the program and simplifies its application, was also incoporated.

Computational procedures

A simplified flowsheet of the computational procedure labelled SIMULATE is presented in Figure 2. This part of the package involves the analysis of the performance of the froth in the plant-scale flotation cell for calculation of the model parameters. The variables are estimated by iterative procedure. However, for the second part of the package (PREDICT), which calculates the performance of a flotation froth under a new set of conditions, the variables are specified as input. The objective functions (OF) that were minimized by a Nelder-Mead (NELM) optimization routine during SIMULATE are briefly summarized in Section 2 of the Addendum.

Application of the program

This section illustrates the application of the computer program to the analysis of the froth in the flotation of fluorspar. The solids in the froth were divided into six size fractions, as indicated in Table 1. Also shown are the mass flowrates of the respective fractions entering the froth and in the concentrate in the plant-scale cell. The former was calculated from the

TABLE 1.
Analysis of the cleaner flotation froth[a] in the first phase of the calculations.

Size, μm	+300	-300 +150	-150 +106	-106 + 75	-75 +45	-45
Mass flowrate into conct., g/s	22	99	96	104	207	582
Mass flowrate into froth, g/s	602	2118	1471	1214	1535	2192
Ratio conct./froth	0,04	0,05	0,07	0,09	0,14	0,27
Ratio to water in tails, kg/kg	0,05	0,19	0,03	0,12	0,10	0,09
Total concentration[b]	12,2	42,9	29,8	24,6	31,1	44,4
- Entrained[b,c]	6,2	22,7	3,3	14,2	12,0	11,4
= Floated[b]	6,0	20,2	26,5	10,4	19,1	33,0

Volumetric ratio of slurry-to-air flow (SLAR) 0,234
Mass flowrate of water entering froth (g/s) 6064

mass flowrate of solids per unit volume of air that enter the froth, as measured on laboratory scale. It was assumed that this parameter stays constant for both the laboratory and the plant cell under similar conditions. The latter was measured on the plant.

Every size class was further divided into two subclasses, viz a floated and an entrained fraction. The fraction that was entrained into the froth was calculated from the ratio of the concentration of each size fraction to the concentration of water in the tailings (assuming that the pulp is perfectly mixed), and the transfer rate of water into the froth (see Table 1). It was assumed that this ratio stays constant, i.e. there is negligible differential classification of the entrained solids and water as they enter the froth.

Material collected from the pulp in a cleaner cell was first floated in a 5-litre Denver laboratory cell, and the aeration rate and the volumetric transfer of slurry into the froth were measured. Analysis of the slurry thus recovered yielded the mass-transfer rates of the various species as well as the ratio of the volumetric flowrate of the slurry to that of the air (SLAR) as they enter the froth. During these tests, the froth was rapidly removed from the surface of the pulp in a simulation of the rate of transfer of material into the froth, i.e. before drainage can occur.

Subsequently, the performance of the cleaner froth was analyzed by experimental measurement of the parameters listed in Table 2. The experimental and predicted velocities at the surface of the froth are presented in Figure 3.

Froth samples of a fixed volume were also taken at different depths in the froth at the point corresponding to x_0 in Figure 1. Analysis of these samples, together with the parameters in Table 2, served as the input to SIMULATE. This algorithm calculated the drainage constant of each subclass from a least-squares regression of the curve of the concentration of the mineral in the plant-scale froth at different

TABLE 2.
Parameters for the cleaner flotation cell.[a]

Length (L) m	Width (W) m	Froth height (H) m	Weir height (z_w) m	Aeration rate (G) m^3/s	ϵ (est.)	F_1 (calc.) m
1,35	1,27	0,27	0,24	0,04	0,69	0,509

Froth breakage parameters: g_{b0} (m/s) $2,78 \times 10^{-2}$
g_{b1} (s^{-1}) $-3,00 \times 10^{-5}$

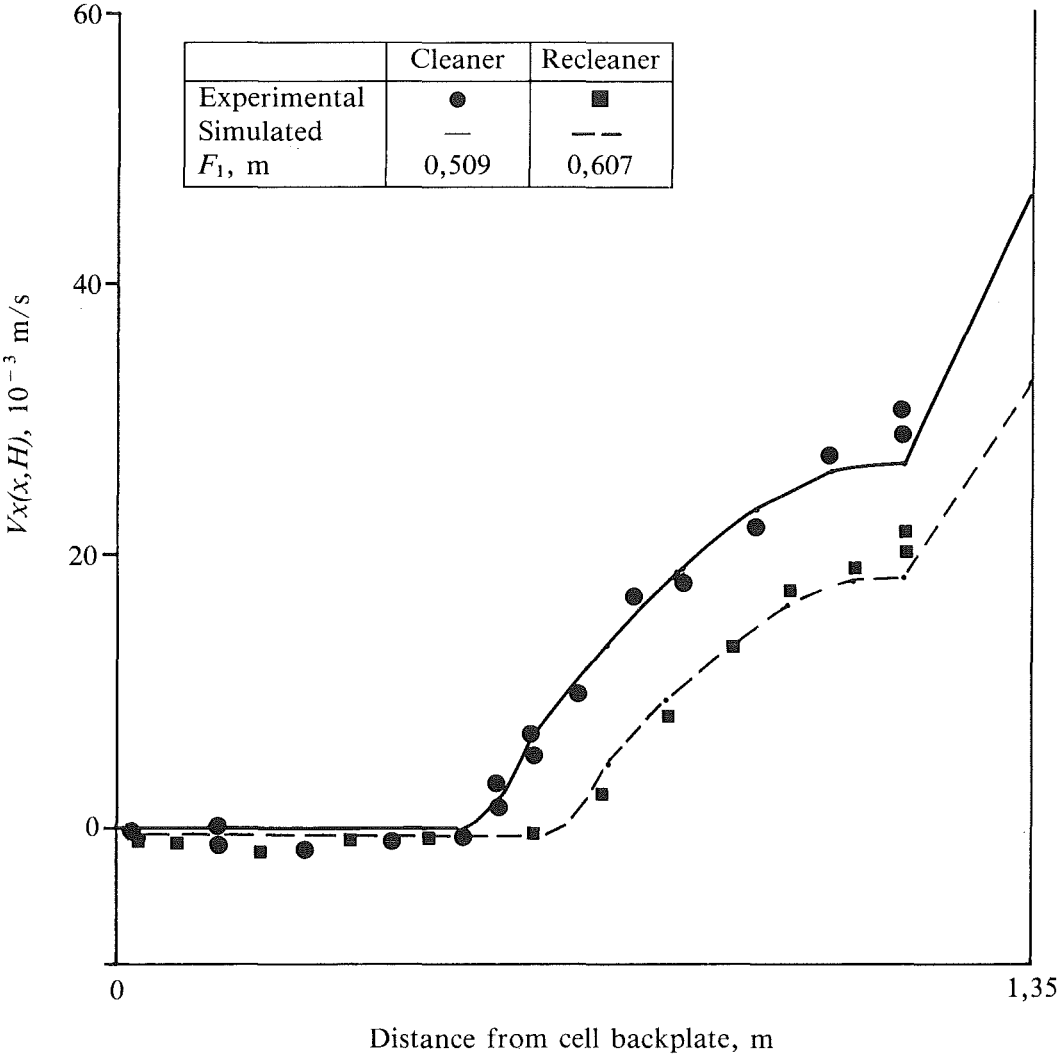

FIGURE 3. Experimental and simulated velocities at the surface of the froth

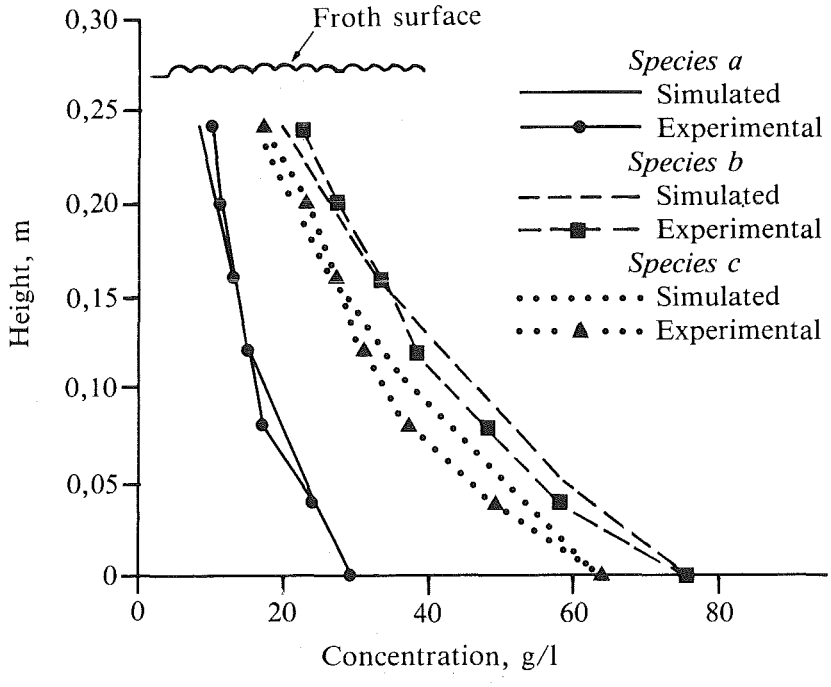

FIGURE 4. Experimental and simulated concentration-height profiles for the froth in the cleaner cell

TABLE 3.

Analysis of the recleaner flotation froth[a] in the first phase of the calculations.

Size, μm	+300	-300 +150	-150 +106	-106 + 75	-75 +45	-45
Mass flowrate into conct., g/s	54	170	120	101	180	426
Mass flowrate into froth, g/s	1328	1443	1073	1014	1597	3281
Ratio conct./froth	0,04	0,19	0,11	0,10	0,11	0,13
Ratio to water in tails, kg/kg	0,17	0,23	0,17	0,14	0,21	0,13
Total concentration[b]	27,6	30,0	22,3	21,3	33,2	68,2
- Entrained[b,c]	22,2	29,6	21,5	18,1	26,7	16,7
= Floated[b]	5,4	0,4	0,8	3,2	6,5	51,5

Mass flowrate of water entering froth (g/s) 6152

Cell data the same as in Table 2, except that ϵ= 0,55, F_1=0,607 m and SLAR = 0,203

Froth breakage parameters: g_{b0} (m/s) 2,99 x 10^{-2}

g_{b1} (s^{-1}) -1,33 x 10^{-4}

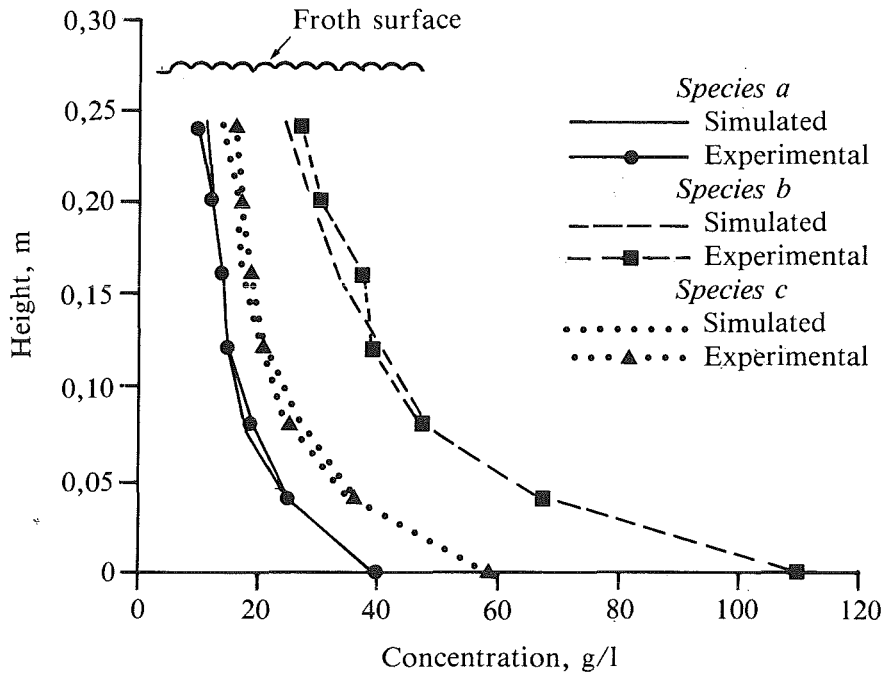

FIGURE 5. Experimental and simulated concentration-height profiles for the froth in the recleaner cell

TABLE 4.
Drainage rate constants (s^{-1}) estimated in SIMULATE from tests on the cleaner and recleaner froths.

Size, μm	Cleaner froth		Recleaner froth	
	Floated	Entrained	Floated	Entrained
+300	0,21	3,82	0,35	8,70
-300+150	0,24	9,52	0,27	15,74
-150+106	0,26	9,51	0,29	16,08
-106+ 75	0,27	5,08	0,30	14,22
- 75+ 45	0,22	7,18	0,30	14,57
- 45	0,25	9,40	0,32	15,02

[a] Denver no.24 D-R cell
[b] Concentration (kg/m^3) in the total volume of slurry and air entering the froth.
[c] Calculated from the ratio of solids to water in the tailings and the flowrate of water into the froth.

heights. This procedure was repeated for a recleaner cell in the fluorspar circuit. The results of this testwork are summarized in Table 3 and the drainage rate constants in both instances are presented in Table 4. The ability of the model to simulate the concentration-height curves at x_0 is shown in Figures 4 and 5. The maximum error between any of the experimental and predicted values is 12% and 7,5% of the measured concentration in the cleaner and recleaner froths respectively.

Sensitivity analysis

The practical implications of the computer program PREDICT in the scale-up of the performance of the froth can best be illustrated by a sensitivity analysis. This is justified because SIMULATE satisfactorily fitted the experimentally measured concentration-height profiles for the industrial froth. Although, in practice, no flotation variable can be altered without simultaneously affecting a host of other variables, the parametric sensitivity of the model can best be illustrated by changing of each variable independently, as was done here. The ability of the model to predict the performance of the cleaner froth when the dimensions of the cell and the operating condi-

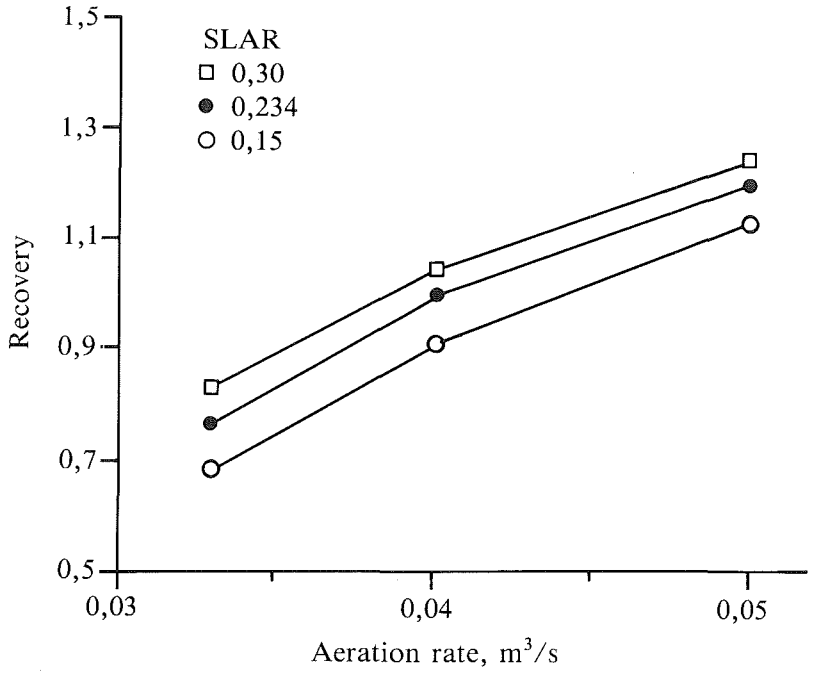

FIGURE 6. The sensitivity of recovery to changes in the rate of aeration

tions are changed during scale-up, is shown in Figures 6 to 10. Recoveries are presented as fractions of the recovery obtained (i.e. 30% of the total recovery in the cleaner bank) for the parameters in Table 2. The drainage rate constants given in Table 4 were used in the predictions.

As expected, recovery increases with an increase in the rate of aeration and in the ratio of slurry to air as they enter the froth, as shown in Figure 6. Under these conditions, the velocity of the froth increases on the surface of the froth towards the concentrate weir and vertically upwards in stage

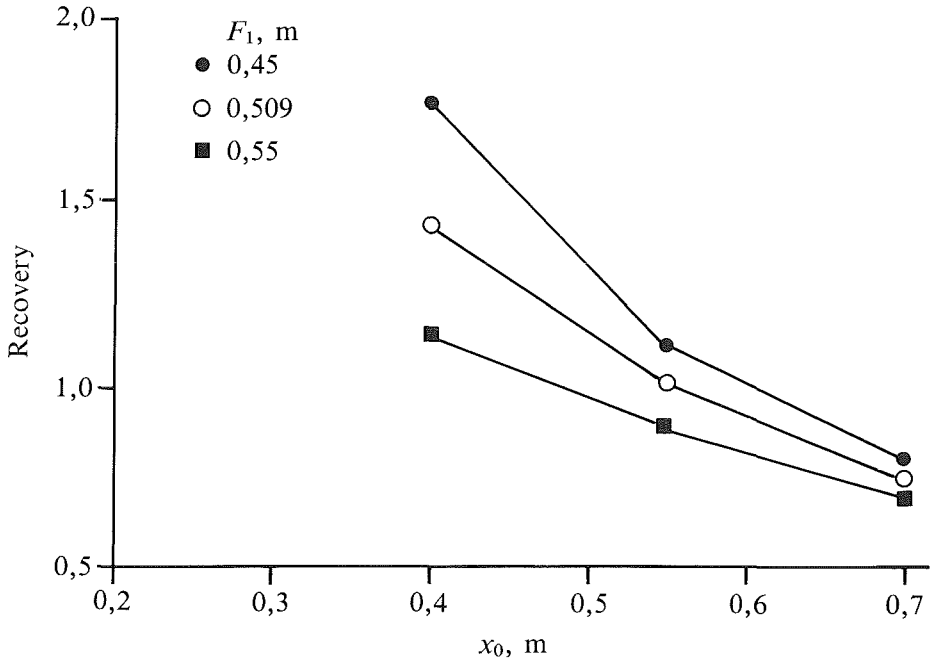

FIGURE 7. The sensitivity of recovery to changes in the inefficient fraction of the froth volume

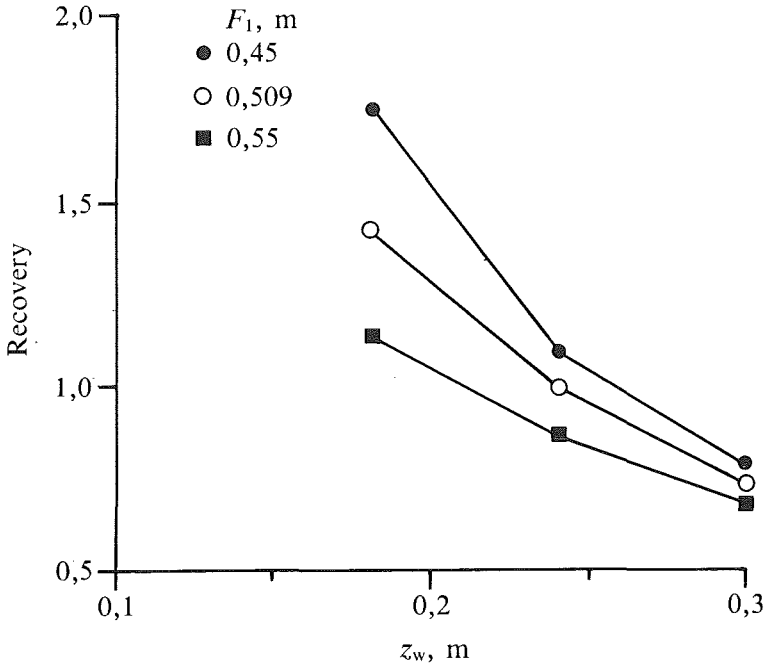

FIGURE 8. The sensitivity of recovery to changes in the height of the concentrate weir

3 if the value of F_1 is constant. A change in the distribution of air in the pulp may affect the inefficient fraction of the froth, denoted by x_0. As indicated in Figure 7, recovery decreases with an increase in the inefficient fraction of the froth. Furthermore, if F_1 increases (i.e. if there is less transfer of froth from stage 2 into stage 3), the recovery decreases if the rate of removal of the concentrate remains constant.

As shown in Figure 8, an increase in the height of the concentrate weir (and the froth column) would result in an overall decrease in the rate of flotation[6] and in the

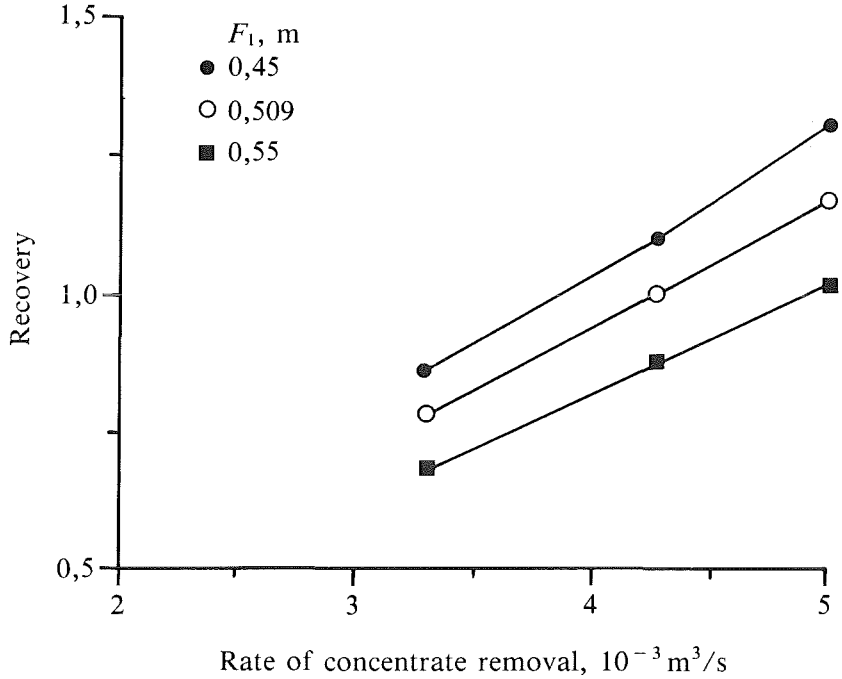

FIGURE 9. The sensitivity of recovery to changes in the rate of concentrate removal

recovery. (The concentration of the particles in the froth decreases with increasing height owing to the drainage of particles.) Furthermore, recovery increases if F_1 decreases (i.e. if there is a greater increase in the velocity in stage 3) and the height of the concentrate weir remains constant.

An increase in the rate of removal of the concentrate with paddles improves the recovery because there is a higher mass flowrate (Figure 9). An increase in the velocity in stage 3 (i.e. a decrease in F_1) also results in an increase in the concentration of material in the froth, and consequently also in the recovery for any given rate of removal of the concentrate. If the length of the cell is increased during scale-up, slower transfer of material into the froth (due to a greater cross-sectional cell area) results in a decrease in recovery, as indicated in Figure 10. However, this may be overcome by an increase in the rate of aeration, because the residence time of particles in the froth is reduced.

This example illustrates the complexity of the interactions between the operating variables, the characteristics of the froth, and the dimensions of the cell, and shows that froth effects should be taken into account during scale-up. Significant deviations from predicted performance can occur if the only relationship considered is that between the pulp residence time in the laboratory and industrial scale cells.

Conclusions

An efficient method has been developed for use in the scale-up of industrial flotation cells from laboratory batch tests. The froth model developed for this purpose incorporates control variables as well as easily measurable froth

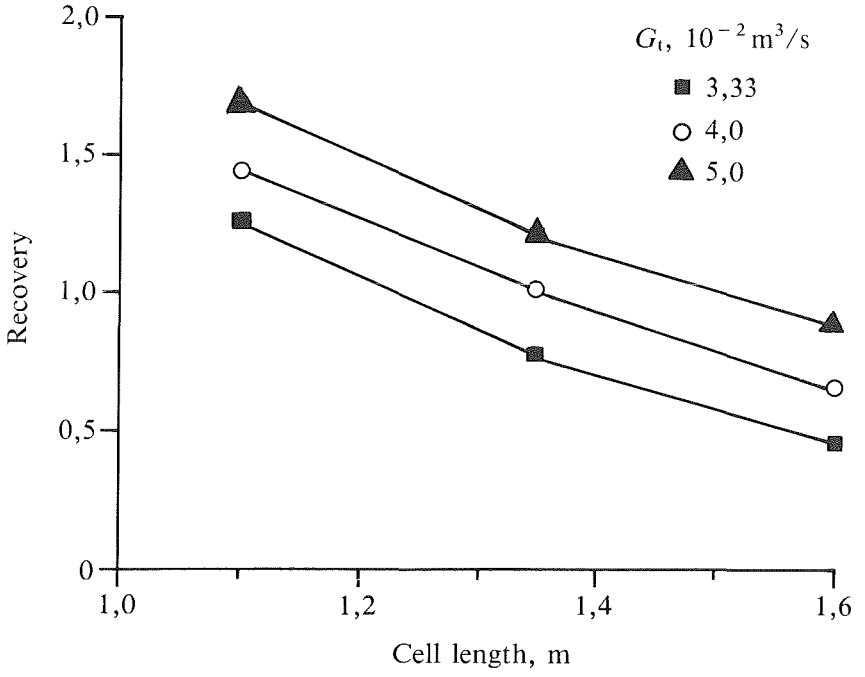

FIGURE 10. The sensitivity of recovery to changes in the length of the flotation cell

characteristics, and permits the froth to be analyzed in terms of its mobility and the drainage constants for the various species in the froth. These parameters are determined experimentally as well as through iterative techniques in the computer program. An advantage of the program is that it can be implemented with ease on a microcomputer.

For both the cleaner and recleaner flotation cells, the programme was found to give an adequate description of the variation in the concentration of the various species in the froth with height above the pulp-froth interface. A sensitivity analysis showed that the model yielded realistic descriptions of changes in operating and design variables due to scale-up. Therefore, when used in conjunction with a model describing the transfer of material from the pulp to the froth, the program could be a powerful tool in the design of industrial cells and in efforts to improve the performance of such cells.

Acknowledgements

This paper is published by permission of the Council for Mineral Technology (Mintek).

References

1. KING, R.P. Simulation of flotation plants. *Trans. Soc. Min. Eng. AIME*. vol. 258, 1975. pp. 286-293.

2. LAPLANTE, A.R., TOGURI, J.M. and SMITH, H.W. The effect of air flow rate on the kinetics of flotation. Part 1: The transfer of material from the slurry to the froth. *Int. J. Miner. Process*. vol. 11, 1983. pp. 203-219.

3. CUTTING, G.W., WATSON, D., WHITEHEAD, A. and BARBER, S.P. Froth structure in continuous flotation cells: Relation to the prediction of plant performance from laboratory data using process models. *Int. J. Miner. Process*. vol. 7, 1981. pp. 347-369.

4. CUTTING, G.W., BARBER, S.P. and NEWTON, S. Effects of froth structure and mobility on the performance and simulation of continuously operated flotation cells. *Int. J. Miner. Process*. vol. 16, 1986. pp. 43-61.

5. KING, R.P., HATTON, T.A. and HULBERT, D.G. Bubble loading during flotation. *Trans. Inst. Min. Metall*. Sect. C, vol. 83, 1974. pp. 112-115.

6. LAPLANTE, A.R., TOGURI, J.M. and SMITH, H.W. The effect of air flow rate on the kinetics of flotation. Part 2: The transfer of material from the froth over the cell lip. *Int. J. Miner. Process*. vol. 11, 1983. pp. 221-234.

7. KALAPUDAS, R. A study on scaling-up of laboratory batch flotation data to industrial size flotation. *XVth INTERNATIONAL*

MINERAL PROCESSING CONGRESS. Paris, Bureau de Recherches Geologiques et Minieres, 1985. vol. 2. pp. 112-121.

8. AGAR, G.E. The optimization of flotation circuit design from laboratory rate data. *XVth INTERNATIONAL MINERAL PROCESSING* CONGRESS. Paris, Bureau de Recherches Geologiques et Minieres, 1985. vol. 2. pp. 100-111.

9. MOYS, M.H. Residence time distributions and mass transport in the froth phase of the flotation process. *Int. J. Miner. Process*. vol. 13, 1984. pp. 117-142.

10. MOYS, M.H. A study of a plug flow model for flotation froth behaviour. *Int. J. Miner. Process*. vol. 5, 1978. pp. 21-38.

Addendum

1. Equations describing the concentration of mineral species and water in stage 2

Floated mineral species i:

$$M_{2fi}(l) = M_{2fi}(0) \qquad l < l_{di}$$

$$= M_{2fi}(0)\ \exp[-(k_{2fi} + k_v)\int_{l_{di}}^{l} dl/V(l)] \qquad l \geq l_{di}$$

where

$M_{2fi}(l)$ = Concentration of species i at distance l along bubble streamline,

$M_{2fi}(0)$ = Concentration of species floated into froth at origin of the streamline

k_{2fi} = Drainage rate constant for floated species i,

k_v = Constant incorporating the variation in the bubble velocity with distance along a streamline, and

l_{di} = Distance along streamline where detachment of floated species from bubble surfaces starts occuring. ($l_{di} = 0$ in this study.)

Entrained mineral species i:

$$M_{2ei}(l) = M_{2ei}(0)\ \exp[-(k_{2ei} + k_v)\int_{0}^{l} dl/V(l)]$$

where the parameters are as described above, but for entrained material. k_{2ei} is the drainage rate constant for entrained species i in stage 2. The same form of equation applies to water.

2. Objective functions for the determination of the model parameters

SIMULATE

(a) F_1 : characteristic constant describing bubble streamlines in stage 2:

$$OF = \sum_{j=1}^{NX2} (v_{xj}{}^{m}(X^*,H) - v_{xj}{}^{p}(X^*,H))^2$$

where NX2 = Number of velocity measurement points on the froth surface. $v_{xj}{}^{m}(X^*,H)$ and $v_{xj}{}^{p}(X^*,H)$ are the measured and predicted surface velocities of the froth respectively.

(b) L' : the boundary of stage 2 nearest to the concentrate overflow weir:

$$OF = (t_{3x} - t_{3z})^2$$

where t_{3x} and t_{3z} are the calculated residence time of froth volumes in stage 3 in a horizontal and vertical direction respectively.

(c) k_{2fi} and k_{2ei} : drainage rate constants for floated and entrained species i:

$$OF = \sum_{All\ j} [M_{2ti}(X_0,Z)_j - (M_{2fi}(X_0,Z)_j + M_{2ei}(X_0,Z)_j + M_{2di}(X_0,Z)_j)]^2$$

where $M_{2fi}(X_0,Z) + M_{2ei}(X_0,Z) + M_{2di}(X_0,Z)$ is the calculated concentration of species i (due to flotation, entrainment, and drainage) in the froth.

$M_{2ti}(X_0,Z)$ is the total measured concentration of species i.

(d) k_{3fi} and k_{3ei} : drainage rate constants in stage 3, incorporating the effects of the action of the froth paddle, turbulence, shear stresses, and bubble coalescence:

$$OF = (M_{ci}{}^{m} - M_{ci}{}^{p})^2$$

where $M_{ci}{}^{m}$ and $M_{ci}{}^{p}$ are the measured and predicted mass flowrates of species i in the concentrate stream respectively.